Electronic Supplementary Information

FeN_x and γ-Fe_2O_3 co-functionalized hollow graphitic carbon nanofibers for efficient oxygen reduction in an alkaline medium

Qiang Yu, [a] Sitian Lian, [a] Jiantao Li, [a] Ruohan Yu, [a, b] Shibo Xi, [c] Jinsong Wu, [b] Dongyuan Zhao, [a] Liqiang Mai [a] and Liang Zhou *[a]

[a] State Key Laboratory of Advanced Technology for Materials Synthesis and Processing, Wuhan University of Technology, Wuhan 430070, P. R. China

[b] Nanostructure Research Centre, Wuhan University of Technologyy, Wuhan 430070, P. R. China

[c] Institute of Chemical and Engineering Sciences, A*STAR (Agency for Science, Technology and Research), Singapore 627833, Singapore

E-mail: liangzhou@whut.edu.cn

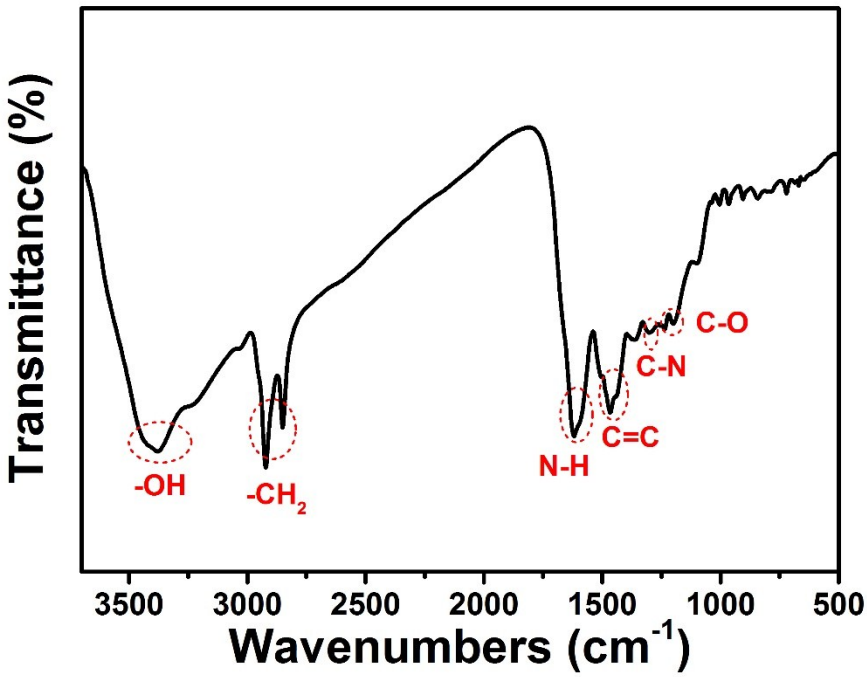

Fig. S1 FTIR spectrum of RNFs.

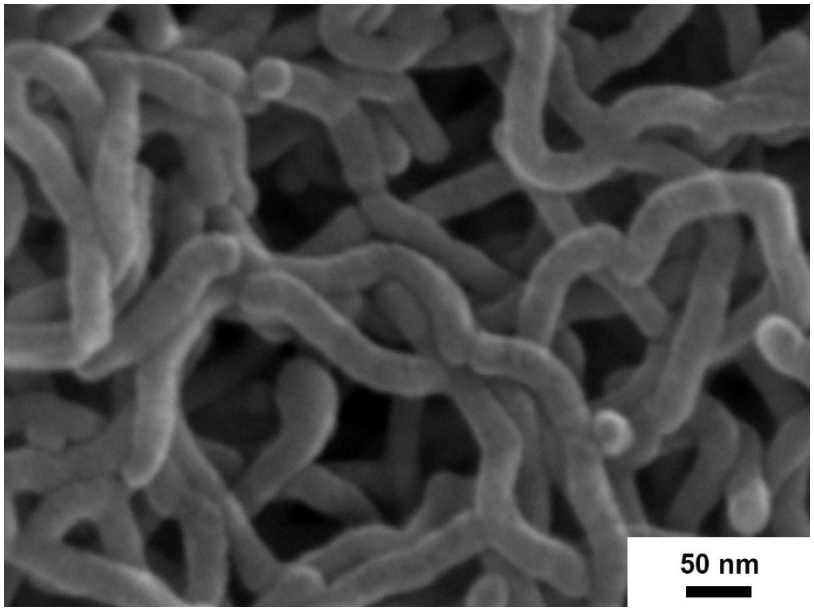

Fig. S2 High magnification SEM image of RNFs.

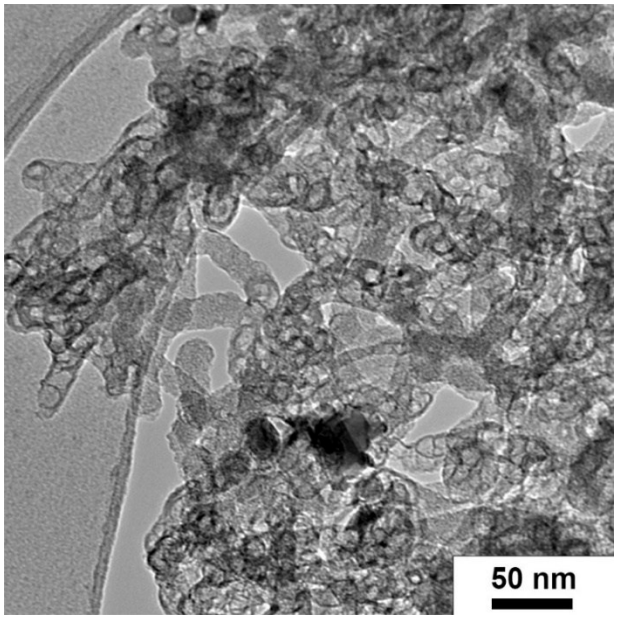

Fig. S3 Low magnification TEM image of FeN_x/Fe_2O_3-CNFs.

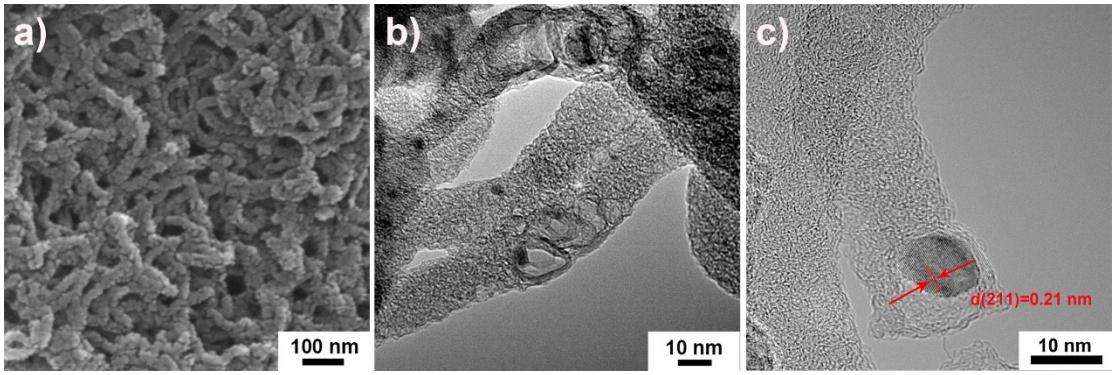

Fig. S4 SEM (a), TEM (b), and HRTEM (c) images of FeN_x/Fe_3C-CNFs.

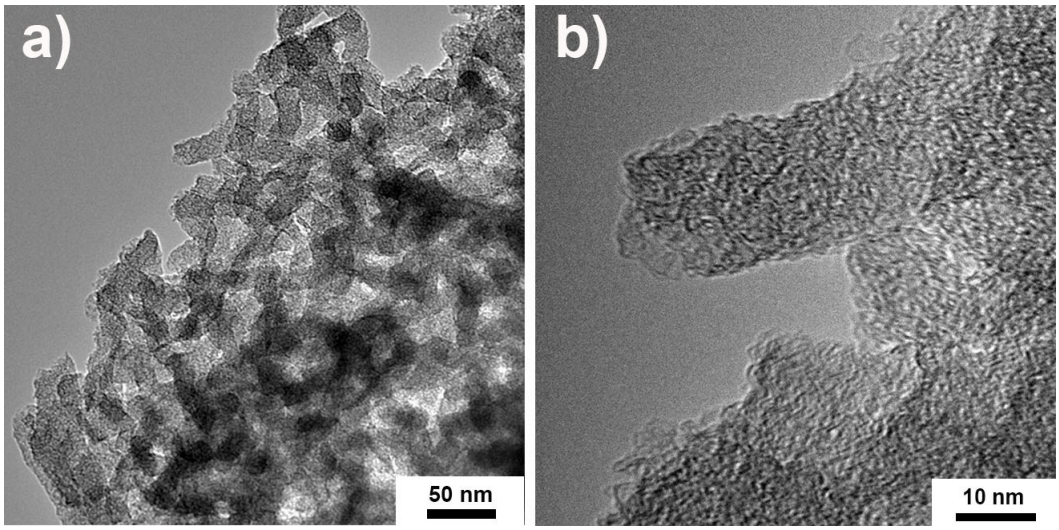

Fig. S5 TEM (a, b) images of N-doped CNFs.

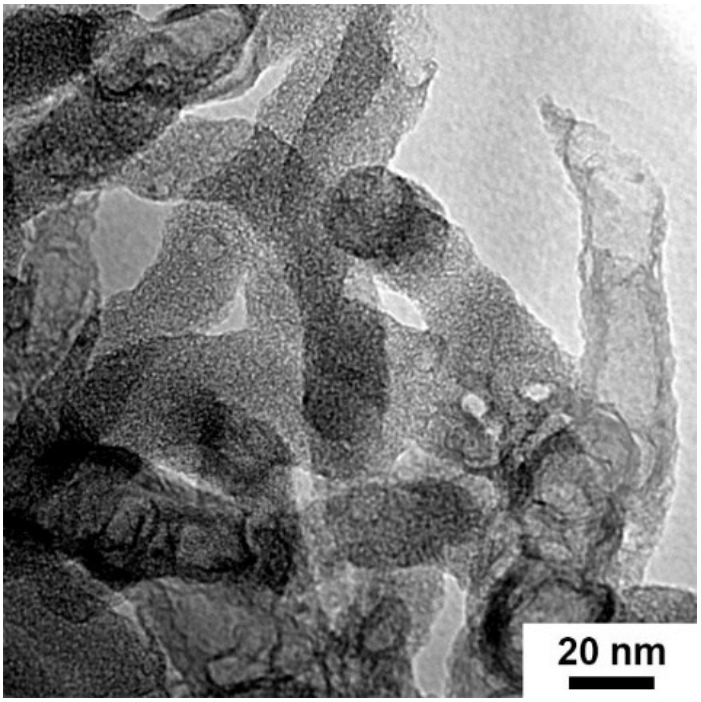

Fig. S6 TEM image of FeN_x/Fe_2O_3-CNFs-700.

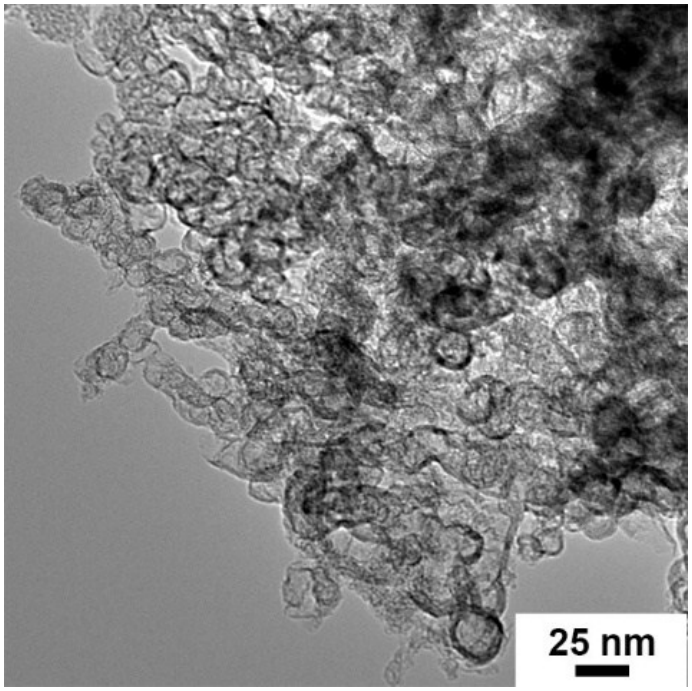

Fig. S7 TEM image of FeN_x/Fe_2O_3-CNFs-900.

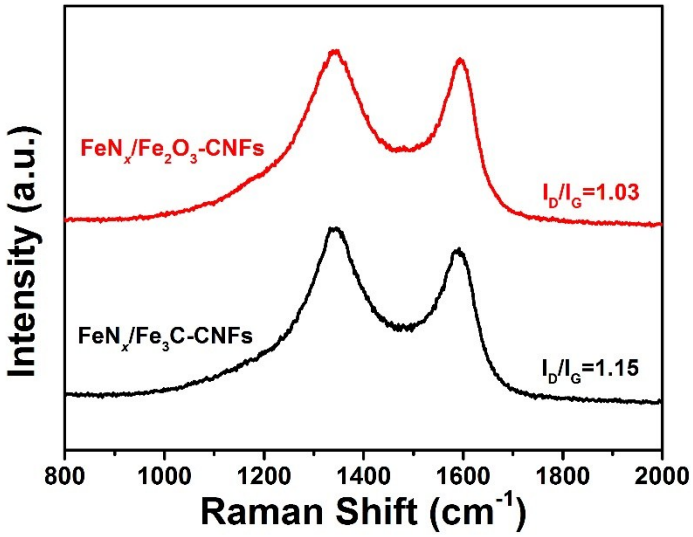

Fig. S8 Raman spectra of FeN_x/Fe_2O_3-CNFs and FeN_x/Fe_3C-CNFs.

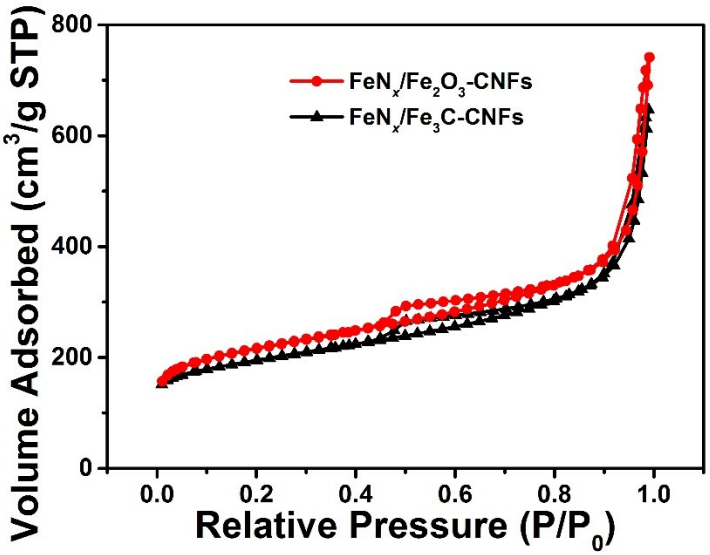

Fig. S9 N_2 adsorption/desorption isotherms of FeN_x/Fe_2O_3-CNFs and FeN_x/Fe_3C-CNFs.

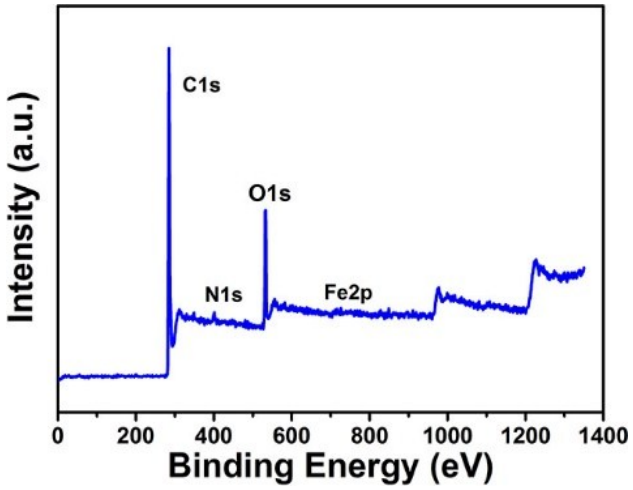

Fig. S10 XPS survey spectrum of FeN_x/Fe_2O_3-CNFs.

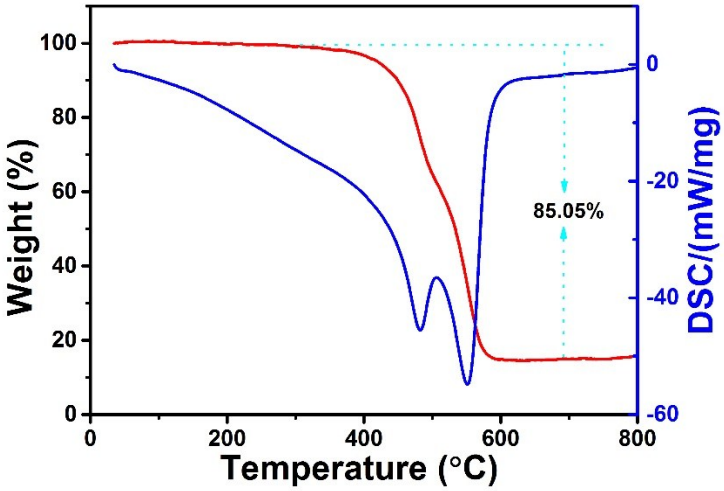

Fig. S11 TG and DSC curves of FeN_x/Fe_2O_3-CNFs.

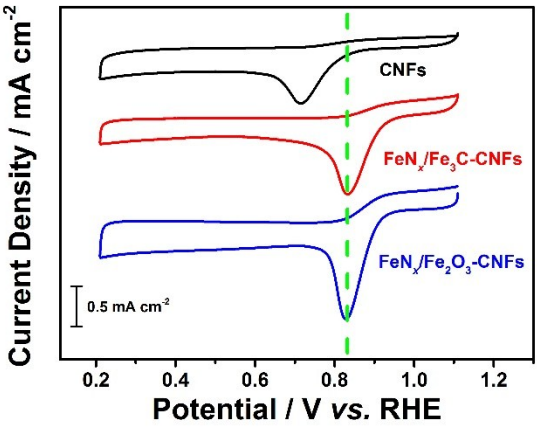

Fig. S12 CV curves of CNFs, FeN_x/Fe_2O_3-CNFs, and FeN_x/Fe_3C-CNFs with a scan rate of 5 mV s^{-1}.

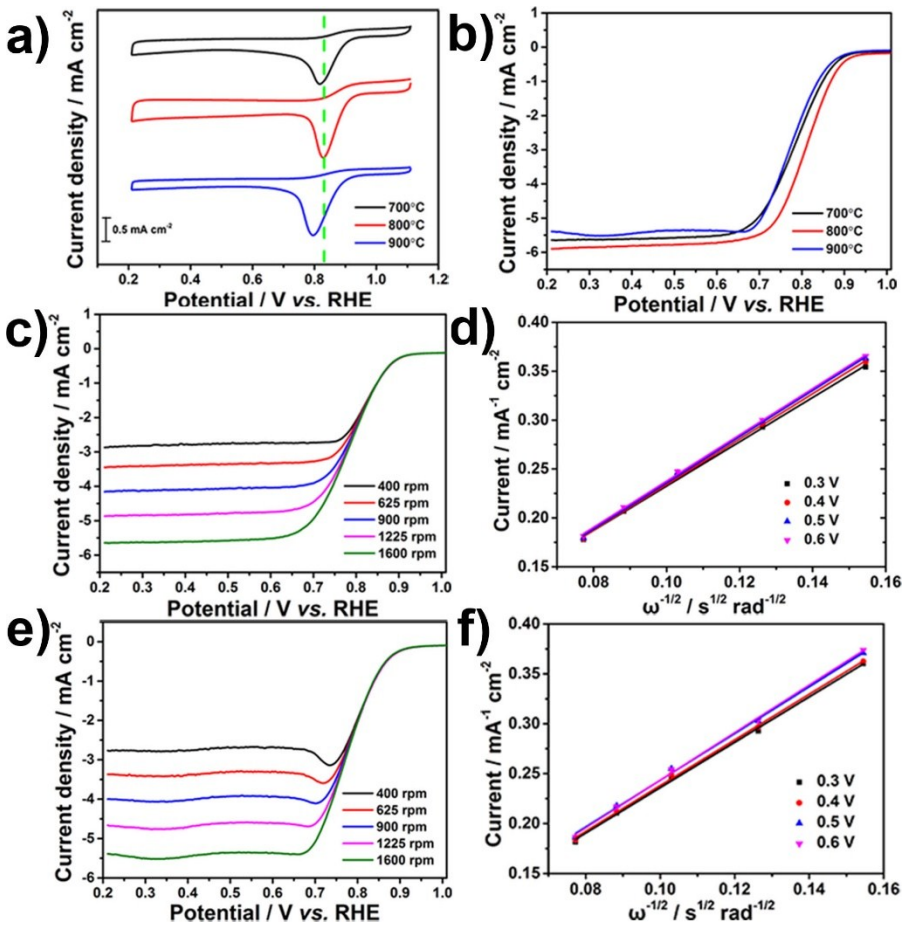

Fig. S13 CV (a) and LSV (b) curves of FeN_x/Fe_2O_3-CNFs catalysts prepared at different activation temperatures; LSV curves (c) and the corresponding K-L plots (d) of FeN_x/Fe_2O_3-CNFs-700; LSV curves (e) and the corresponding K-L plots (f) of FeN_x/Fe_2O_3-CNFs-900.

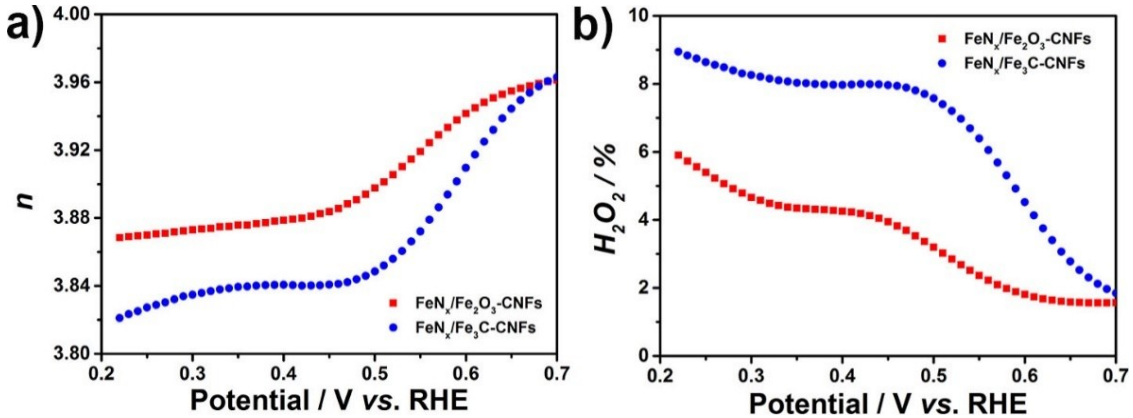

Fig. S14 Electron transfer number (a) and H_2O_2 yields (b) of FeN_x/Fe_2O_3-CNFs and FeN_x/Fe_3C-CNFs at 0.2 – 0.7 V.

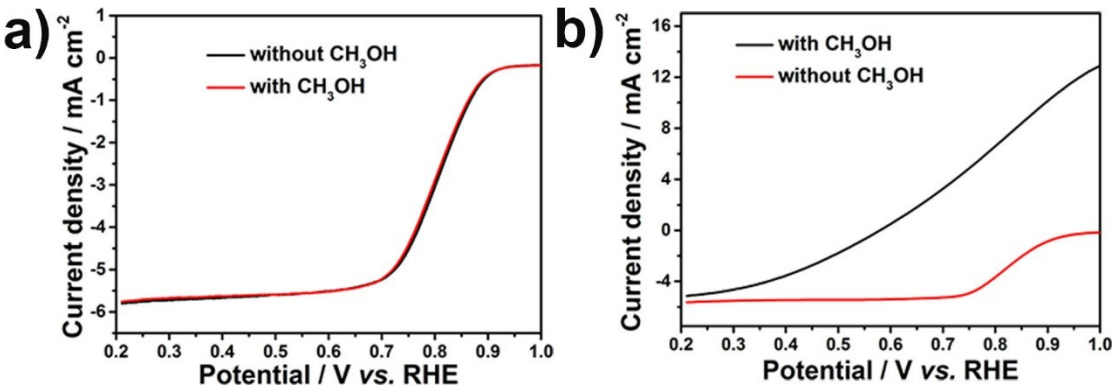

Fig. S15 LSV curves of FeN_x/Fe_2O_3-CNFs (a) and Pt/C (b) with and without CH_3OH.

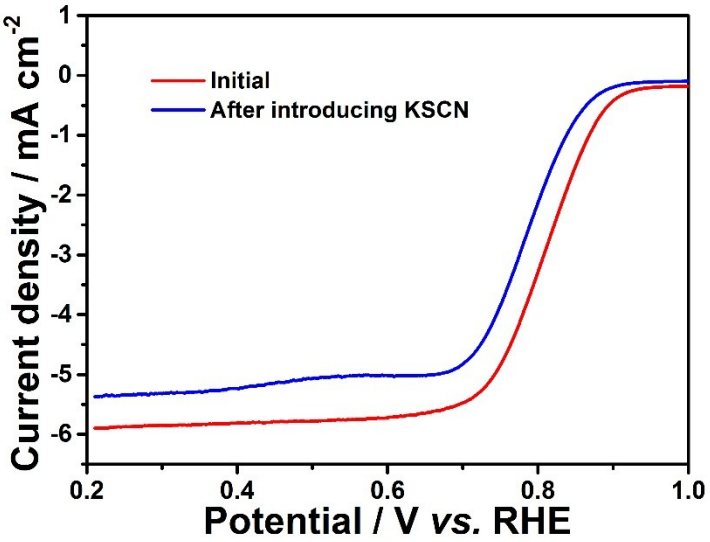

Fig. S16 Effect of SCN^- on the catalytic activity of FeN_x/Fe_2O_3-CNFs.

Table S1. Textural properties of the samples.

Sample	S_{BET} ($m^2\ g^{-1}$)	$S_{t\text{-Plot Micro}}$ ($m^2\ g^{-1}$)	V_p ($cm^3\ g^{-1}$)	$V_{t\text{-Plot Micro}}$ ($cm^3\ g^{-1}$)
FeN_x/Fe_2O_3-CNFs - 700	679	299	1.43	0.15
FeN_x/Fe_2O_3-CNFs - 800	712	308	1.15	0.16
FeN_x/Fe_2O_3-CNFs - 900	1093	160	2.36	0.07
FeN_x/Fe_3C-CNFs - 800	639	279	1.00	0.14
CNFs	408	308	0.34	0.15

Table S2. Summary of the Mössbauer site parameters to different iron species in FeN_x/Fe_2O_3-CNFs catalysts.

Fe species	CS ($mm\ s^{-1}$)	D ($mm\ s^{-1}$)	A	W+ ($mm\ s^{-1}$)	Content (%)
Doublet 1	0.86	2.01	15900	0.37	15.7%
Doublet 2	0.35	0.58	39400	0.35	39%
Sextet 1	0.31	0.04	28000	0.27	27.7
Sextet 2	1.05	-0.06	17700	0.60	17.5%

CS: Center shift; D: Quadrupole splitting; A: Area; W+: Absorption line width

Table S3. Comparison of the ORR performance of non-precious metal catalyst in 0.1 M KOH at 1600 rpm.

Sample	Onset potential (V vs. RHE)	Half-wave potential (V vs. RHE)	J_{Limit} @0.4 V ($mA\ cm^{-2}$)	$J_{Kinetic}$ @0.9 V ($mA\ cm^{-2}$)	Reference
FeN_x/Fe_2O_3-CNFs	0.95	0.81	~6	0.50	This work
p-Fe-N-CNFs	0.91	0.82	5.05	/	1
PFA-Fe5-900-ALP	0.92	0.85	5.4	/	2
N-doped carbon tube	0.89	0.76	~4.9	~0.26	3
Fe-N/C-800	0.98	0.81	4.81	~0.32	4
Fe-N-CNFs	0.93	0.81	5.12	/	5
Co-N-doped Graphitic carbon	0.92	0.82	5.3	~0.32	6
FeCo/N-doped carbon aerogels	0.89	0.81	~6	~0.13	7
B-doped Fe−N_x centers-enriched porous carbons	0.97	0.84	5.5	~0.93	8
MOG(Fe)/urea/CNTs-700	0.92	0.72	5.37	~0.11	9
α-Fe_2O_3/CNT	0.82	/	~4	/	10
Fe/N/S-PCNT	0.96	0.84	~5	~0.55	11
Graphene-like carbon nanosheets	0.86	0.77	4.8	/	12

1. B. C. Hu, Z. Y. Wu, S. Q. Chu, H. W. Zhu, H. W. Liang, J. Zhang and S. H. Yu, *Energy Environ. Sci.*, 2018, **11**, 2208-2215.

2. L. C. Pardo Pérez, N. R. Sahraie, J. Melke, P. Elsässer, D. Teschner, X. Huang, R. Kraehnert, R. J. White, S. Enthaler, P. Strasser, and A. Fischer, *Adv. Funct. Mater.,* 2018, 1707551.
3. W. Wei, H. T. Ge, L. S. Huang, M. Kuang, A. M. Al-Enizi, L. J. Zhang and G. F. Zheng, *J. Mater. Chem. A,* 2017, **5**, 13634-13638.
4. W. H. Niu, L. G. Li, X. J. Liu, N. Wang, J. Liu, W.J. Zhou, Z. H. Tang, and S. W. Chen, *J. Am. Chem. Soc*., 2015, **137**, 5555.
5. Z. Y. Wu, X. X. Xu，B. C. Hu，H. W. Liang, Y. Lin, *Angew. Chem. Int. Ed.,* 2015, **54**, 8179.
6. S. H. Liu, Z. Y. Wang, S. Zhou, F. J. Yu, M. Z. Yu, C. Y. Chiang, W. Z. Zhou, J. J. Zhao, and J. S. Qiu, *Adv. Mater*., 2017, 1700874.
7. G. T. Fu, Y. Liu, Y. F. Chen, Y. W. Tang, J. B. Goodenough and J. M. Lee, *Nanoscale,* 2018, **10**, 19937-19944.
8. K. Yuan, S. Sfaelou, M. Qiu, D. Lützenkirchen-Hecht, X. D. Zhuang, Y. W. Chen, C. Yuan, X. L. Feng, and U. Scher, *ACS Energy Lett.,* 2018, **3**, 252-260.
9. H. Wang, X. C Cheng, F. X. Yin, B. H. Chen, T. Y. Fan, X. B. He, *Electrochim. Acta,* 2017, **232**, 114–122.
10. M. Sun, Y. Z. Dong, G. Zhang, J. H. Qu and J. H. Li, *J. Mater. Chem. A,* 2014, **2**, 13635.
11. Z. Tan, H. X. Li, Q. X. Feng, L. L. Jiang, H. Y. Pan, Z. Y. Huang, Q. Zhou, H. H. Zhou, S. Ma, Y. F. Kuang, *J. Mater. Chem. A,* 2019, **7**, 1607-1615.
12. C. Hu, Y. Zhou, R. Ma, Q. Liu and J. Wang, *J. Power Sources*, 2017, **345**, 120-130.